

Structure-dependent deuterium release from ion implanted beryllium: comparison between Be(1 1 $\bar{2}$ 0) and Be(poly)

M. Oberkofler, M. Reinelt, S. Lindig, Ch. Linsmeier *

*Max-Planck-Institut für Plasmaphysik, EURATOM Association, Boltzmannstr. 2,
85748 Garching b. München, Germany*

Abstract

The temperature-driven release of deuterium implanted as keV ions into metallic beryllium is measured by temperature programmed desorption (TPD). TPD spectra from single and polycrystalline Be implanted with 1 keV ions are compared. The high temperature desorption stage ($T > 700$ K) is attributed to the release of deuterium trapped at several types of energetically different ion-induced defects. A release peak around 850 K is recorded in the single crystal, while in the polycrystal all deuterium desorbs below this temperature. An increase in the maximum release temperature is observed after implantation of the polycrystal with higher ion energies (2 and 3 keV). We propose an interpretation of the experimental results based on two types of traps, with depth distributions adapted to the implantation energy. Preliminary TMAP7 calculations qualitatively reproduce the shifts in the maximum desorption temperature, observed in the polycrystal at different implantation energies. The difference between the single and the polycrystal is explained by a higher density of surviving defects in the single crystal. Diffusion of mobile defects to grain boundaries and subsequent annihilation is proposed as the dominant mechanism for

differences in deuterium desorption from Be(11 $\bar{2}$ 0) and Be(poly).

Keywords: Beryllium; Deuterium Inventory; Implantation; Trapping; Defects; Thermal Desorption

PACS codes: 61.80.Jh; 61.72.Hh; 68.43.Vx; 68.55.Ln; 82.20.Pm

* Corresponding author, Tel.: +49-89-32992285, Fax.: +49-89-3299962285, Email: linsmeier@ipp.mpg.de

1 Introduction

Metallic beryllium is planned as an inner vacuum vessel cladding for the international fusion experiment ITER, covering an area of 690 m² of the plasma-facing first wall[1]. During operation with a deuterium or a deuterium / tritium plasma, the first wall materials are subjected to elevated heat loads and energetic particle fluxes of hydrogen isotopes (D and T at energies from eV to keV and fluences greater than $1 \times 10^{17} \text{ cm}^{-2}$). This leads to implantation and accumulation of hydrogen in the material far from thermodynamic equilibrium. To control fuel balancing and minimize the retention of radioactive T in the plasma vessel, the temperature-dependent recycling process is of great concern. Because the impinging particle flux not only forces hydrogen into beryllium, but also removes the hydrogen-enriched surface layers by physical sputtering, a steady state concentration is eventually reached. This concentration, however, depends on temperature, because diffusive processes transport hydrogen further inside the bulk, as well as towards the surface, releasing it back into the plasma. The surface temperature of the Be is expected to range from room temperature up to the melting point (during off-normal events such as disruptions). The planned bake-out temperature for ITER is 530 K. The thermal release ('outgassing') of implanted hydrogen depends strongly on the binding energy of hydrogen to the metal matrix. High activation energies for desorption (above 1 eV) can be associated to the release of hydrogen from traps with high binding energies. Detrapping into mobile states occurs at correspondingly high temperatures. Investigations of the thermal release of implanted deuterium from single crystalline and chemically pure Be show a number of binding states with a fluence-dependent occupation. Release peaks

are recorded at temperatures of 440, 470, 770 and 840 K[2]. Diffusion of D through unirradiated Be is fast at room temperature with an activation barrier of only 0.29 eV[3], as it is common for most metals. Therefore, the peaks in the TPD spectra can be attributed to release of D from irradiation-induced traps. The experimentally investigated systems consist purely of Be and D. Thus, the nature of the traps only depends on the structure of the Be-D material (with possible formation of beryllium hydride[4],[5]). To gain further information about the nature of the different sites, we compare the thermal release of D implanted into single and polycrystalline Be substrates at different ion energies. In this way we vary the depth distribution of the defects generated in the collision cascades, as well as the available sinks (surface and grain boundaries) for mobile defects. We present experimental results and discuss an interpretation based on TMAP7 modelling.

2 Experimental procedures

The results from temperature-programmed desorption (TPD) studies on single crystals (sc) have been published before[2,4]. Experimental details for the polycrystal (pc) measurements are identical. In brief, a polished sc disc (diameter of 14 mm, thickness less than 1 mm, and $(1\bar{1}\bar{2}0)$ surface orientation) and a polished pc sample ($10.5 \times 10.5 \times 0.5$ mm 3) are sputter-cleaned by 3 keV Ar $^+$ bombardement and subsequently annealed up to 1000 K to gain sub-monolayer oxygen coverage as the only remaining impurity visible by in-situ performed X-ray photoelectron spectroscopy (XPS). These well established surfaces are then implanted with deuterium ions at room temperature. The sc Be sample is implanted with a 3 keV monoenergetic and mass-selected D $_3^+$ beam up to a

fluence of $2 \times 10^{17} \text{ D cm}^{-2}$. Instantaneous dissociation of the molecule at the surface can be assumed, resulting in an effective energy per D atom of 1 keV. The pc sample is implanted in the same way with a 3 keV or 6 keV D_3^+ or a 6 keV D_2^+ beam to obtain energies per atom of 1, 2, and 3 keV, respectively.

The samples are then heated to 1000 K with a linear temperature ramp and the desorbing species are recorded with a quadrupole mass spectrometer (QMS) positioned in line-of-sight geometry in front of the sample. The TPD spectra shown in this work are recorded at 4 amu/e, corresponding to D_2 . Other deuterium-containing species are either not observed during TPD (D, HDO, D_2O) or show a signal intensity more than one order of magnitude lower than molecular deuterium (as in the case of HD). Hence, it can be assumed that deuterium desorbs as D_2 molecules.

The temperature ramps for the TPD experiments are 1 K/s for the sc and 0.73 K/s for the pc. From measurements with a ramping rate of 1.34 K/s on the pc sample (not shown) it can be inferred that the difference in the temperature ramps does not account for the main effects in the comparison of pc and sc observed in this work. In order to exclude an influence of the sample history, the desorption of 1 keV implanted deuterium from the pc was carried out at the beginning of the experimental campaign and again repeated at the end of it. The spectra perfectly match, therefore no influence of the experimental series on the conditions of the pc sample and hence the resulting TPD spectra is observed.

After the last annealing cycle the samples were investigated ex situ by electron backscattered diffraction (EBSD) mapping. These measurements were performed in a field emission gun scanning electron microscope (Helios FEI)

using a Norlys II detector (HKL / Oxford Instruments). For the single crystal, the recorded Kikuchi patterns confirmed the $(1\bar{1}\bar{2}0)$ orientation of the surface. The averaged relative deviation from this orientation is significantly lower than 0.5° over the examined area of $128 \times 128 \mu\text{m}^2$. The results for the polycrystal are shown in figure 1. The colours correspond to different orientations of crystallites. Three reference orientations are assigned the primary colours red, green and blue; other orientations result in secondary colours. A band contrast picture is overlaid to the colour map. In this picture the contrast of the Kikuchi patterns is assigned a grayscale, yielding darker pixels where the patterns are more diffuse. Grain boundaries are thus highlighted. Grains up to $20 \mu\text{m}$ in diameter with various orientations are visible.

3 TPD measurements

Figure 2 shows TPD spectra from single and polycrystalline beryllium respectively, implanted with 1 keV D. Two distinct temperature regions of deuterium release can be identified. For the single crystal the broad high temperature release stage has been assigned to deuterium detrapping from defect sites, created upon irradiation[2,4]. This is in agreement with the finding that irradiation-induced defects in beryllium strongly influence the lattice site occupation of implanted impurities[6], especially of deuterium[7]. We call these traps 'ion induced', as they originate from the collision cascade initiated by ions hitting the metal surface. The more sharply peaked release stage around 450 K appears only at higher fluences. The threshold fluence for the occurrence of this low-temperature release stage lies around $1 \times 10^{17} \text{ cm}^{-2}$ for both the single and the polycrystal. It has been argued[2,4] that deuterium released in this

temperature regime originates from supersaturated ($\text{Be}/\text{D} > 0.4$), and thereby structurally modified Be-D areas. The TPD spectrum from the polycrystal, just as the one from the single crystal, also shows the two mentioned distinct release stages. Still, some differences can be noticed. First, the ratio between the integrated areas of the high and low temperature regimes differs between the single and the polycrystal. This difference indicates that in the polycrystal a bigger fraction of the retained deuterium is released from supersaturated areas. Yet this might not be an effect of the difference in crystallinity, as it could be caused by differences in the implantation beam profile. Secondly the release from the ion induced traps happens at lower temperatures in the polycrystal as compared to the single crystal. An interpretation of this shift of the high temperature edge of the spectra is presented in section 4.

Figure 3 shows TPD spectra from the polycrystalline sample after implantation with deuterium ions at energies of 1, 2 and 3 keV per atom. The spectra vary slightly, the most prominent difference being a shift in the high temperature edge of the release from ion induced traps. The shift amounts to 50 K between the implantations with 1 and 2 keV per atom, and another 25 K between the implantations with 2 and 3 keV. Assuming various trap sites in the implanted material, different peaks in the TPD spectra can be assigned to detrapping from sites with different activation energies. Thus a shift in the highest desorption temperature could be explained by a change in the nature of the traps, e.g. different sizes of clustered vacancies. However, it is also possible to explain such a shift by assuming unaltered traps (i.e. activation energies) and instead adapting the depth distribution of the traps to the respective implantation energy. In the following section we present a plausibility model taking into account energy-dependent density profiles of ion

induced traps. This model is implemented in TMAP7[8]. This code includes treatments of temperature transport, trapping, diffusion and surface recombination. The results of TMAP7-simulated TPD spectra are compared to the observed temperature shifts in the experimental TPD spectra at different implantation energies.

4 Discussion of the high-temperature edge shift

Upon irradiation of beryllium with 1, 2 or 3 keV deuterium, a large number of Frenkel pairs is created in collisional cascades. Molecular dynamics simulations show that a large fraction of these Frenkel pairs has recombined by the time the cascade has cooled down (for a review see for example [9] and [10]). At maximum primary knock-on energies of 600 eV (for 1 keV D on Be) to 1800 eV (for 3 keV D on Be) the surviving defects are primarily point defects, i.e. single vacancies or self interstitials. Irradiation-induced defects have been shown to be mobile in beryllium at room temperature[11,12] and can therefore diffuse to sinks such as the surface or grain boundaries to annihilate, or face annihilation upon encountering an anti-defect. Some defects will be trapped by forming immobile impurity-defect complexes with the implanted projectile[13], preferably at the end of the collision cascade. Deuterium atoms implanted into beryllium have been shown to be trapped near the site where they are stopped[14]. A depth distribution of trapped deuterium can therefore be calculated using of the Monte Carlo simulation program SDTrim.SP[15,16]. This program is an extension of the TRIM code[17] to allow for material accumulation (and erosion) in the implanted sample. It is based on the binary collision approximation and considers a deuterium projectile to be stopped in

the beryllium when its kinetic energy falls below a given cut-off energy (here 2 eV) due to energy losses. The resulting implantation profile for each implantation energy can roughly be approximated by a Gaussian, truncated due to the intersection with the surface. The maxima of the fitted Gaussians lie at 37 nm (1 keV), 66 nm (2 keV) and 94 nm (3 keV), their root mean square deviations being 21 nm, 30 nm and 33 nm respectively. These profiles are used as input for the TMPA7 simulations.

Moreover, some of the point defects will form clusters (dislocation loops or fine cavities, as observed for example by Yoshida et al.[18] and Chernikov et al.[19]). These represent a second kind of trap for diffusing deuterium atoms. At fluences of 10^{17} atoms cm^{-2} , as applied in our experiments, hundreds of collision cascades will overlap spatially. Cascades produced in the debris of earlier cascades will heal parts of the clustered defects and their density will eventually saturate. In the qualitative picture drawn here, by the end of the implantation a constant density of surviving defect clusters will have evolved up to a depth that can be estimated from the range of a Frenkel defect depth profile, accessible again by a calculation with SDTrim.SP. As this depth varies with the energy of the incident deuterium, the total number of these traps also scales with the implantation energy. After implantation, and before the onset of a TPD experiment, these cluster traps may be empty or partially filled with deuterium. During a TPD experiment, however, they are assumed to be filled up by retrapping of some of the deuterium released from traps with lower activation energies, such as those in the low-temperature region of the shown spectra.

The above considerations can be summarized in the following model. We assume two kinds of ion induced traps responsible for the high temperature

release stage of the TPD spectra. The first kind arises from a deuterium atom merging with a nearby defect at the implantation site, directly after it is stopped. A second kind of traps is represented by small defect clusters. The density of these traps is assumed to be constant, up to a depth dependent on the Frenkel pair depth profile (and therefore of the energy of the implanted deuterium) and zero beyond that depth.

In a first attempt to simulate the TPD spectra of the polycrystal shown in figure 3, the trap profiles (both dependent on the implantation energy) are used as input to the program TMAP7. All traps are assumed to be saturated with deuterium at the onset of the high temperature release stage. The clustered defects are assigned a somewhat higher activation energy than the implantation sites. The resulting spectra clearly show a shift in the high temperature edge as a function of implantation energy. The shift is of the right order of magnitude (50 K and 25 K) and about twice as big between the 1 keV and the 2 keV implanted spectra than between the 2 keV and the 3 keV implanted spectra. This model would also provide an explanation for the spectra recorded by Markin et al.[20], where the highest release temperature reaches up to 1000 K for beryllium implanted with deuterium at an energy per atom of 5 keV. The absolute release temperatures in the simulations are still different from the experiment, indicating that some of the TMAP7 input parameters need further optimization. The reproduction of the temperature shift, however, demonstrates the validity of the defect distribution assumption.

It is realized and emphasized that the illustrated model is oversimplified. For example, any evolution of the microstructure during the heating of the samples is neglected. Nevertheless, the simulations show the possibility to explain the shift in the high temperature edge of the TPD spectra by simply adapting im-

plantation and damage profiles to the used implantation energy. No additional traps with different detrapping energies are needed in our model for the 2 keV and 3 keV implanted TPD spectra as compared to the 1 keV implanted. The identical activation energies are applicable to all three implantation energies. It is important to notice that two consequences of varying the implantation energy cause the shift. First, the larger range of the vacancy cluster traps for higher implantation energy - the trap density being held constant over this range - implies a larger total amount of such traps, available for deuterium atoms to be trapped in. Second, the fact that the trap profiles are shifted further into the bulk for higher implantation energies results in a longer path towards the surface for detrapped atoms before they can recombine and desorb. The simulations reveal that the latter effect is smaller than the first. It should be mentioned here, that, as discussed in [2], surface recombination is not considered to be a rate limiting step for the release of D implanted into Be.

Now we turn to the comparison of the polycrystal with the single crystal. We see from figure 2 that there is a shift in the maximum temperature at which release is observed in TPD measurements. Assuming the same nature of traps in both specimens, we try an interpretation based on the difference in crystallinity. The implantation profiles and Frenkel defect production during the collision cascades can be considered to be independent of crystallinity. However, grain boundaries have been shown to play an important role in the evolution of the initially generated defects. Several authors (among others, Hudson et al.[21], Norris[22] and Zinkle et al.[23]) have observed zones denuded of voids near grain boundaries in various irradiated materials. Singh et al.[24] calculated a decrease in void concentration with decreasing grain size

in austenitic stainless steel irradiated with 1 MeV electrons. We therefore assume a reduced trap density in the irradiated pc beryllium as compared to the sc: Single defects created upon irradiation might diffuse to grain boundaries of the pc where they face annihilation. Moreover, stresses originating from the misorientation at grain boundaries in the pc might attract defect clusters otherwise immobile in the sc. On the contrary, in the sc, mobile defects could survive longer and travel further until they finally form immobile compounds. These mechanisms lead to an increased defect density, and thus, to a higher number of available traps for deuterium in the sc. Deuterium might possibly even be trapped at greater depths than in the pc due to the greater distance defects can travel without annihilating at grain boundaries. Our TMAP7 calculations have shown that both an increased number of traps, as well as their distribution deeper into the bulk contribute to a shift of the highest release peak observed in TPD spectra towards higher temperatures. It is therefore possible, that the shift observed in the comparison of the TPD spectra from the single and the polycrystal in figure 2 is due to differences in the defect evolution depending on the absence or presence of grain boundaries.

5 Summary

The retention behaviour of deuterium implanted polycrystalline beryllium is compared to that of the single crystal. In both cases, release takes place in two stages. The sharp low temperature peak is attributed to deuterium trapped in regions where the beryllium lattice is structurally modified due to supersaturation. It only appears above a fluence of $1 \times 10^{17} \text{ cm}^{-2}$. At higher temperatures deuterium is released from non-supersaturated regions where it is trapped in

ion-induced defect sites.

For the observed shift of the high-temperature edge to lower temperatures in the case of the polycrystal as compared to the single crystal, a possible explanation is proposed. This shift could be the consequence of a reduced density of the traps with the highest activation energy. A possible mechanism leading to such a reduction is the diffusion of vacancies towards grain boundaries in the polycrystal.

In the polycrystal sample, it is observed that upon raising the implantation energy, the high-temperature edge of the TPD spectrum shifts to higher temperatures. On the basis of a model with two kinds of traps and trap distributions which depend on the implantation energy, this feature can be qualitatively reproduced in simulations, without changing the nature (i.e. the activation energies) of the traps.

References

- [1] J. Roth, E. Tsitrone, and A. Loarte. Plasma-wall interaction: a complex combination of surface processes critical for thermo-nuclear fusion. *Journal of Physics: Conference Series*, 100(6):062003, 2008.
- [2] M. Reinelt and Ch. Linsmeier. Temperature programmed desorption of 1 kev deuterium implanted into clean beryllium. *Physica Scripta*, T128:111–114, 2007.
- [3] E. Abramov, M. P. Riehm, D. A. Thompson, and W. W. Smeltzer. Deuterium permeation and diffusion in high-purity beryllium. *J. Nucl. Mater.*, 175(1-2):90–95, December 1990.
- [4] M. Reinelt, A. Allouche, M. Oberkofler, and Ch. Linsmeier. Retention

mechanisms and binding states of deuterium implanted into beryllium.

Submitted to New Journal of Physics.

- [5] G. De Temmerman. Insight into the codeposition of deuterium with beryllium: influence of the deposition conditions on deuterium retention and release. To be submitted to *Journal of Nuclear Materials*.
- [6] J. Hanßmann, O. Meyer, and G. Linker. Influence of vacancy mobility and volume size mismatch energy on the lattice site occupation of implanted species in beryllium single crystals. *Nuclear Instruments and Methods in Physics Research Section B: Beam Interactions with Materials and Atoms*, 122(4):635–638, March 1997.
- [7] R. Vianden, E. N. Kaufmann, and J. W. Rodgers. Impurity lattice location in ion-implanted beryllium: Measurements and systematics. *Phys. Rev. B*, 22(1):63, July 1980.
- [8] J.A. Ambrosek and G.R. Longhurst. Verification and validation of tmap7. Technical Report INEEL/EXT-04-01657, Idaho Falls, September 2004.
- [9] Bachu Singh. Damage production, accumulation and materials performance in radiation environment. *Journal of Computer-Aided Materials Design*, 6(2):195–214, May 1999.
- [10] T. Diaz de la Rubia, N. Soneda, M. J. Caturla, and E. A. Alonso. Defect production and annealing kinetics in elemental metals and semiconductors. *Journal of Nuclear Materials*, 251:13–33, November 1997.
- [11] J. C. Nicoitd, J. Delaplace, J. Hillairet, D. Schumacher, and Y. Adda. Etude des defauts crees dans le beryllium par irradiation a basse temperature. *Journal of Nuclear Materials*, 27(2):147–165, August 1968.
- [12] J. Delaplace, J.C. Nicoud, D. Schumacher, and G. Vogl. Low-temperature neutron radiation damage and recoveryl in beryllium. *Phys. Stat. Sol.*, 29:819,

1968.

- [13] W.R. Wampler. Trapping of deuterium in beryllium. *Journal of Nuclear Materials*, 196-198:981–985, December 1992.
- [14] V. Kh. Alimov, V. N. Chernikov, and A. P. Zakharov. Depth distribution of deuterium atoms and molecules in beryllium implanted with d ions. *Journal of Nuclear Materials*, 241-243:1047–1051, February 1997.
- [15] W. Eckstein. *Computer Simulation of Ion-Solid Interactions*, volume 10 of *Springer Series in Materials Science*. Springer, Berlin, 1991.
- [16] W. Eckstein, R. Dohmen, A. Mutzke, and R. Schneider. Sdtrimsp: A monte carlo code for calculating collision phenomena in randomized targets. Report IPP 12/3, IPP, 2007.
- [17] J. P. Biersack and L. G. Haggmark. A monte carlo computer program for the transport of energetic ions in amorphous targets. *Nuclear Instruments and Methods*, 174(1-2):257–269, 1980.
- [18] N. Yoshida, S. Mizusawa, R. Sakamoto, and T. Muroga. Radiation damage and deuterium trapping in deuterium ion injected beryllium. *Journal of Nuclear Materials*, 233-237(Part 2):874–879, October 1996.
- [19] V. N. Chernikov, V. Kh. Alimov, A. N. Markin, and A. P. Zakharov. Gas swelling and related phenomena in beryllium implanted with deuterium ions. *J. Nucl. Mater.*, 228(1):47–60, February 1996.
- [20] Andrey V. Markin, Vladimir N. Chernikov, Sergey Yu. Rybakov, and Andrey P. Zakharov. Thermal desorption of deuterium implanted into beryllium. *Journal of Nuclear Materials*, 233-237(Part 2):865–869, October 1996.
- [21] J. A. Hudson, D. J. Mazey, and R. S. Nelson. Void formation in nickel during 20 mev c++ irradiation at 525 °c. *Journal of Nuclear Materials*, 41(3):241–256, December 1971.

- [22] D. I. R. Norris. The use of the high voltage electron microscope to simulate fast neutron-induced void swelling in metals. *Journal of Nuclear Materials*, 40(1):66–76, July 1971.
- [23] S. J. Zinkle and K. Farrell. Void swelling and defect cluster formation in reactor-irradiated copper. *Journal of Nuclear Materials*, 168(3):262–267, December 1989.
- [24] B. N. Singh and A. J. E. Foreman. Calculated grain size-dependent vacancy supersaturation and its effect on void formation. *Philosophical Magazine*, 29(4):847–858, 1974.

Fig. 1. EBSD map of the surface of the polycrystalline sample. The orientation of crystallites is colour-coded. Grain boundaries appear dark due to overlay of a band contrast picture.

Fig. 2. TPD spectra from D-implanted single and polycrystalline Be. The samples were implanted at room temperature up to a fluence of $2 \times 10^{17} \text{ D cm}^{-2}$. The energy per implanted atom was 1 keV. The signal of the quadrupole mass spectrometer at $m/e = 4$ (corresponding to D_2) is plotted against the temperature of the sample surface. The temperature ramping rates are 0.73 K/s and 1 K/s respectively. This difference in ramps does, however, not account for the observed shift of the highest recorded release temperature.

Fig. 3. TPD spectra from polycrystalline Be implanted with D at various ion energies. The samples were implanted at room temperature up to a fluence of $2 \times 10^{17} \text{ D cm}^{-2}$. The signal of the quadrupole mass spectrometer at $m/e = 4$ (corresponding to D_2) is plotted against the temperature of the sample surface. The temperature ramping rate is 0.73 K/s.

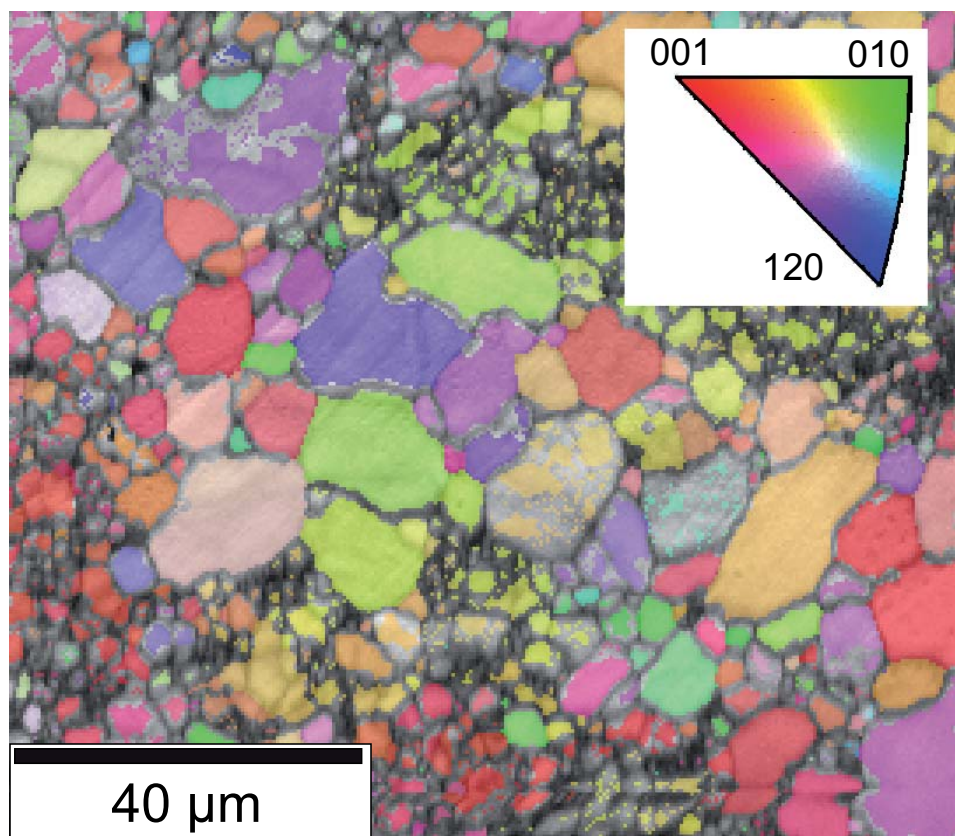


Fig. 1, Oberkofler et al., D retention in Be materials

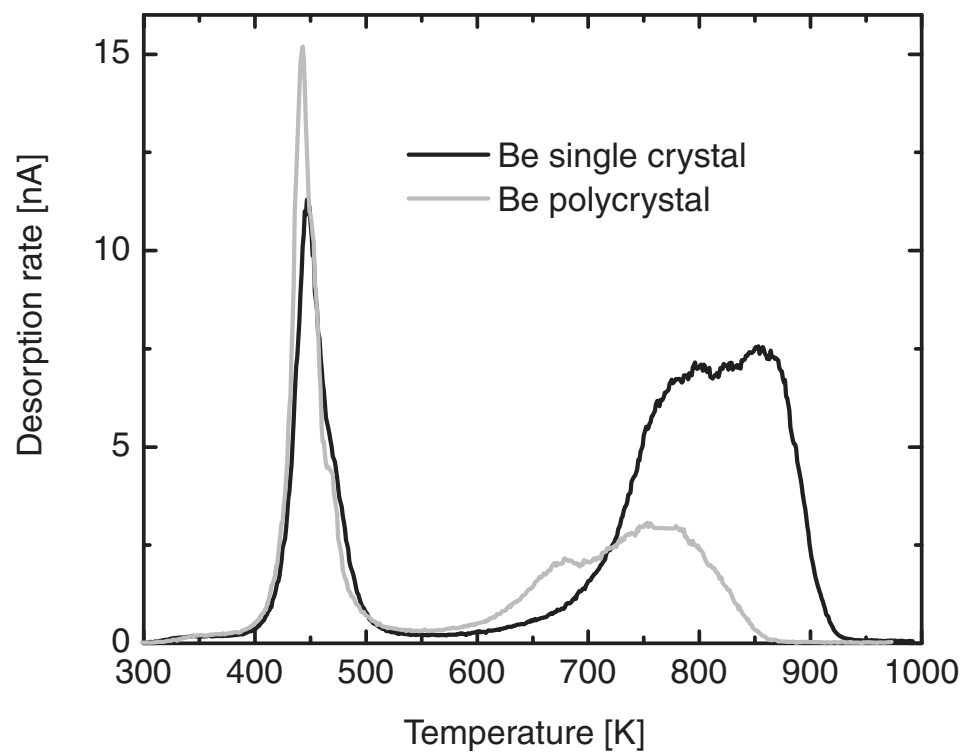


Fig. 2, Oberkofler et al., D retention in Be materials

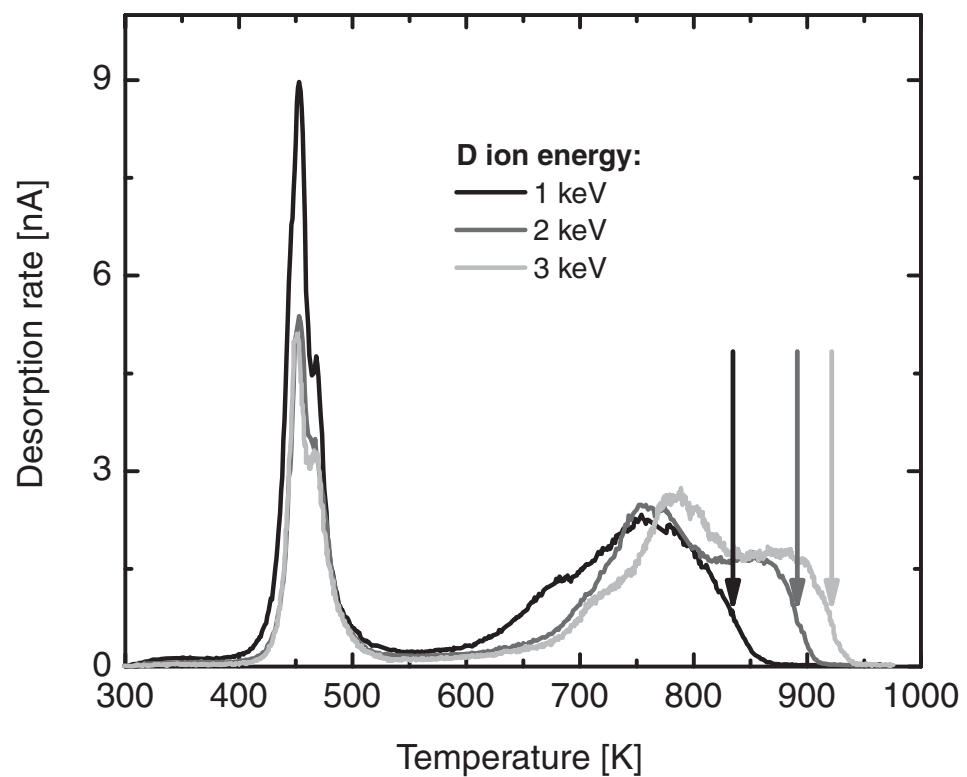


Fig. 3, Oberkofler et al., D retention in Be materials